

# Journal Pre-proof

Conjugation of soy protein isolate (SPI) with pectin by ultrasound treatment

Xiaobin Ma, Furong Hou, Huanhuan Zhao, Danli Wang, Weijun Chen, Song Miao, Donghong Liu



PII: S0268-005X(20)30034-5

DOI: <https://doi.org/10.1016/j.foodhyd.2020.106056>

Reference: FOOHYD 106056

To appear in: *Food Hydrocolloids*

Received Date: 6 January 2020

Revised Date: 7 May 2020

Accepted Date: 26 May 2020

Please cite this article as: Ma, X., Hou, F., Zhao, H., Wang, D., Chen, W., Miao, S., Liu, D., Conjugation of soy protein isolate (SPI) with pectin by ultrasound treatment, *Food Hydrocolloids* (2020), doi: <https://doi.org/10.1016/j.foodhyd.2020.106056>.

This is a PDF file of an article that has undergone enhancements after acceptance, such as the addition of a cover page and metadata, and formatting for readability, but it is not yet the definitive version of record. This version will undergo additional copyediting, typesetting and review before it is published in its final form, but we are providing this version to give early visibility of the article. Please note that, during the production process, errors may be discovered which could affect the content, and all legal disclaimers that apply to the journal pertain.

© 2020 Published by Elsevier Ltd.

## **Author statement**

Xiaobin Ma: experimental investigation, data processing, original draft preparation

Furong Hou: experimental investigation

Huanhuan Zhao: paper reviewing and editing

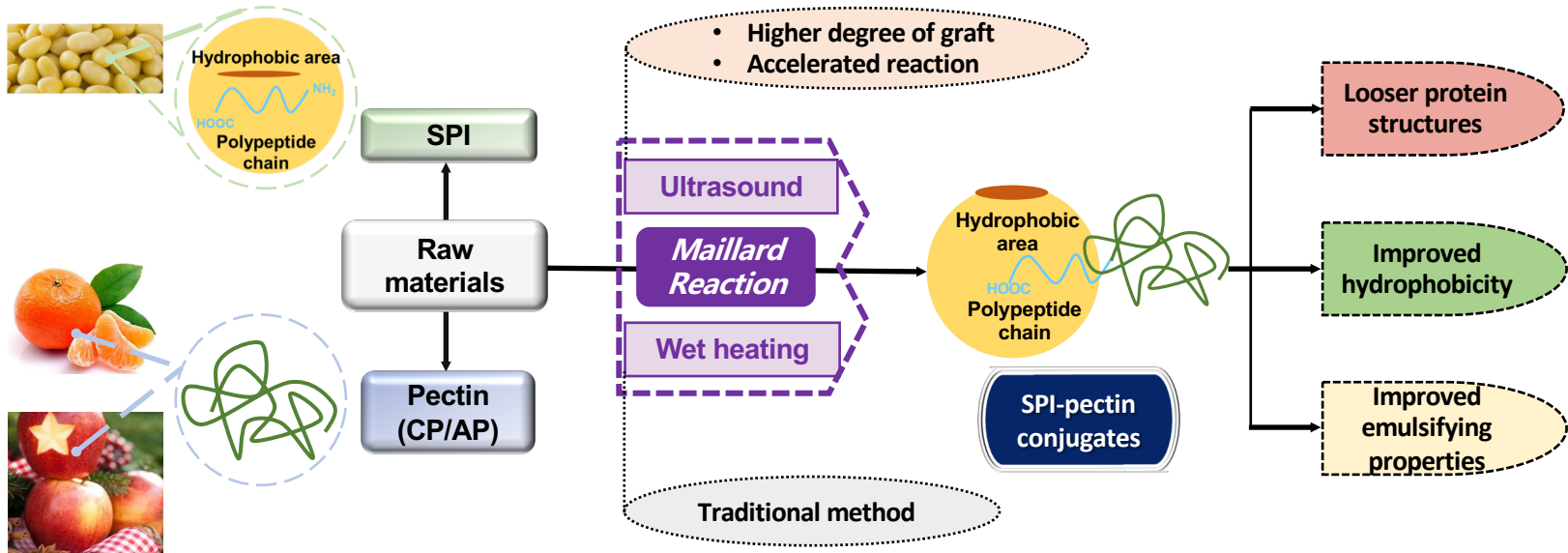
Danli Wang: experimental investigation

Weijun Chen: paper reviewing

Song Miao: paper reviewing

Donghong Liu: supervision

Journal Pre-proof





19 **Abstract**

20 The Maillard reaction in the aqueous system with and without ultrasound  
21 treatment was used to prepare conjugates between soy protein isolate (SPI) and citrus  
22 pectin (CP) / apple pectin (AP). Ultrasound treatment at a power of 450 W and a  
23 temperature of 70 °C significantly accelerated the conjugation processes between SPI  
24 and pectin samples and led to much greater grafting extents compared to the  
25 traditional wet heating. A higher degree of graft of the SPI-CP conjugates was  
26 achieved at a shorter ultrasound duration compared to the SPI-AP conjugates,  
27 possibly attributed to the larger molecular weight and the more flexible structure of  
28 AP. SDS-PAGE analysis confirmed the formation of SPI-pectin conjugates. Analysis  
29 of the protein secondary and tertiary structures suggested that the attachment of CP or  
30 AP changed the spatial conformation of SPI and led to a looser protein structure. In  
31 addition to the grafting process, ultrasound was also observed to play a marked role in  
32 unfolding the SPI resulting in more favorable structures for the Maillard reaction.  
33 Furthermore, the application of ultrasound to the conjugation process significantly  
34 increased the surface hydrophobicity and emulsifying properties of both conjugates,  
35 indicating that ultrasound can be a desirable method for protein-polysaccharide  
36 conjugation.

37 **Keywords:** ultrasound; wet heating; soy protein isolate; pectin; structure; emulsifying  
38 property

39

## 40 1. Introduction

41 In the past few decades, O/W emulsions stabilized by proteins have been  
42 extensively introduced as a useful delivery system (Nooshkam & Varidi, 2019). It is  
43 these emulsions that food and pharmaceutical scientists have used over the years to  
44 protect lipophilic active compounds against environmental stress or degradation,  
45 allow for controlled release, and cover up an unpleasant smell or taste (Bouyer,  
46 Mekhloufi, Rosilio, Grossiord, & Agnely, 2012). However, the main challenge raised  
47 by the use of such protein-stabilized emulsions is lack of stability, given that they are  
48 prone to coalescence, creaming and phase separation that can be induced by a series  
49 of factors such as extreme pH, temperature and ionic strength (Yang, et al., 2015). To  
50 overcome these techno-functional issues, recently scientists have focused on  
51 anchoring polysaccharides onto oil droplet surfaces by the use of a simple Maillard  
52 reaction (Nooshkam & Varidi, 2019).

53 The Maillard reaction is an umbrella term for a complex group of reactions  
54 between an amino acid and a reducing sugar, which can produce various colored and  
55 volatile products (Yu, Seow, Ong, & Zhou, 2017). The early stage of Maillard reaction  
56 involves an initial condensation of the carbonyl group of a reducing sugar with an  
57 amino group of the protein, resulting in the formation of Schiff base. It then  
58 undergoes Amadori rearrangements and a range of reactions and finally turns into  
59 melanoidins that gives the brown color to food matrices. These advanced products  
60 however can be very harmful, and have been reported to cause various diseases  
61 including diabetes and Alzheimer's (Silván, Assar, Srey, Del Castillo, & Ames, 2011).

62 This has led increasing research effort to the application of polysaccharides to the  
63 Maillard reaction. Compared to mono- and oligosaccharides, polysaccharides have  
64 relatively weaker reducibility and stronger molecular steric hindrance, which could  
65 restrict the advanced reactions and thus reduce the undesired products (de Oliveira,  
66 Coimbra, de Oliveira, Zuñiga, & Rojas, 2016; Zhang, et al., 2019). The formation of  
67 protein-polysaccharide conjugates also combines the merits of these two  
68 biomacromolecules together, resulting in unique characteristics such as the excellent  
69 solubility, improved emulsifying properties and higher stability against various  
70 environmental conditions (Nooshkam & Varidi, 2019).

71 Today, most protein-polysaccharide conjugates are simply prepared via dry  
72 heating without extra substrates. However, this method involves a lyophilization  
73 process prior to the reaction and requires controlled temperature and humidity, leading  
74 to the high cost for industrial applications (de Oliveira, et al., 2016; Zhang, et al.,  
75 2019). In addition, the relatively moderate conditions (60 °C) and lack of medium  
76 generally result in very slow reactions that could last for several weeks (Zhang, et al.,  
77 2019). In this case, some researchers start to conduct Maillard reaction in aqueous  
78 mediums, where the conjugation time can be shortened by increasing the reaction  
79 temperature, though protein denaturation also easily occurs (Zhang, et al., 2019). This  
80 is why diverse non-thermal processing techniques, including ultrasound (Li, Huang,  
81 Peng, Shan, & Xue, 2014; Qu, et al., 2018), pulsed electric field (Guan, et al., 2010)  
82 and high pressure (Xu, et al., 2010), are increasingly introduced to the traditional  
83 Maillard reaction.

84           Among these non-thermal processing techniques studied thus far, ultrasound is of  
85 particular interest because of its unique cavitation effect, *i.e.* the rapid formation,  
86 growth and collapse of gas bubbles. It has been shown that ultrasound could  
87 accelerate the Maillard reaction and improve the grafting extent; further, it also  
88 proved effective in altering the structures of protein-polysaccharide conjugates  
89 resulting in more desirable functionality (Qu, et al., 2018). As supported by Li, et al.  
90 (2014), a degree of graft (DG) of peanut protein isolate (PPI)–glucomannan  
91 conjugates of 30.15% was achieved with ultrasound treatment for 80 min, whereas it  
92 took 40 h for classical wet heating to obtain a similar DG. Furthermore, ultrasound  
93 treatment was also observed to improve the solubility and emulsifying properties of  
94 the conjugates. Similar findings have also been reported for the rapeseed protein  
95 isolate (RPI)-dextran (Qu, et al., 2018) and PPI-maltodextrin (Chen, Chen, Wu, & Yu,  
96 2016) conjugates prepared by ultrasound.

97           In this work, soy protein isolate (SPI) and two pectin samples, *i.e.* citrus pectin  
98 (CP) and apple pectin (AP), were selected as the raw material for conjugation. As an  
99 ideal protein product that contains more than 90% protein, SPI has received extensive  
100 research interest for its low cost and desirable nutritional and functional properties  
101 (Wang, et al., 2008). Likewise, pectin is also a low-cost plant material with 85.5%  
102 commercial source from citrus peel and 14.0% from apple pomace (Chan, Choo,  
103 Young, & Loh, 2017); its excellent gelling, stabilizing and emulsifying properties  
104 have made it a promising material for the food industry. In the previous work (Ma, et  
105 al., 2020) we have studied the Maillard reaction between SPI and CP/AP in the dry



106 state, where the SPI-CP and SPI-AP conjugates were obtained at 60 °C and a relative  
107 humidity of 79% for 5 days, achieving the DG of 25.00% and 21.85%, respectively.  
108 As ultrasound offers possibility of enhancing the conjugation process within shorter  
109 period of time, in this study we will employ the high-intensity ultrasound to prepare  
110 the SPI-pectin conjugates. On the other hand, currently, the systematic research  
111 involves in the Maillard reaction between protein and polysaccharide under an  
112 ultrasonic field, including the effects of different operational factors, structural  
113 changes, and relevant functionality improvements of the conjugates is still deficient,  
114 since only a small amount of studies regarding these aspects have been published (Qu,  
115 et al., 2018). Therefore in this study, our objectives are to investigate the effects of  
116 ultrasound conditions (e.g. power, temperature, time) on SPI-pectin conjugation, to  
117 analyze the quantitatively structural changes of conjugates that occurred at the  
118 secondary and tertiary levels, and to illuminate the implications of these changes on  
119 the emulsifying properties of the resulting conjugates. Furthermore, the performance  
120 of traditional wet heating and ultrasound treatment in preparing conjugates, as well as  
121 the properties of conjugates produced by different pectin samples, will be compared  
122 to provide references on both method and material aspects for innovative food  
123 emulsifier design.

## 124 **2. Materials and Methods**

### 125 **2.1. Materials**

126 Defatted soybean meal was obtained from Hengrui Food Ltd. (Guangzhou,  
127 China). Citrus pectin (P9135), apple pectin (93854) and

128 8-Anilino-1-naphthalenesulfonic acid (ANS) were purchased from Sigma–Aldrich  
129 (Shanghai, China). Sodium-dodecyl-sulfate polyacrylamide gel (SDS-PAGE) kit was  
130 purchased from Beyotime Biotechnology (Shanghai, China). All other reagents  
131 including o-Phthaldialdehyde (OPA), sodium azide, SDS, etc., were purchased from  
132 Sinopharm Chemical Reagent Co., Ltd. (Shanghai, China).

## 133 **2.2. Preparation of SPI**

134 Preparation of SPI was carried out according to our previous studies (Ma, et al.,  
135 2020; Ma, et al., 2019). The final protein content was  $96.22 \pm 0.48$  (%).

## 136 **2.3. Analysis of molecular information of pectin**

137 The weight-average molecular weight ( $M_w$ ), number-average molecular weight  
138 ( $M_n$ ), polydispersity ( $M_w/M_n$ ), z-average root mean square (RMS) radius of gyration  
139 ( $R_z$ ) and intrinsic viscosity  $[\eta]$  were measured through a size exclusion  
140 chromatography (SEC) combined with a multi-angle laser light scattering (MALLS,  
141 Wyatt Dawn Heleos-II, USA) system, equipped with a refractive index detector  
142 (RID-10A, Shimazu Corporation, Kyoto, Japan) and an on-line differential viscometer  
143 (ViscoStarTMII, Wyatt Technology, USA). The mobile phase was 0.2 M NaCl  
144 solution (containing 0.02%  $\text{NaN}_3$ ) and used to dissolve pectin samples to obtain a  
145 concentration of  $3 \text{ mg mL}^{-1}$ . Solutions were stirred overnight and then filtered through  
146 a  $0.22 \mu\text{m}$  membrane before loading. The flow rate, elution time and  $\text{dn/dc}$  value were  
147 set at  $0.75 \text{ mL min}^{-1}$ , 90 min and  $0.1355 \text{ mL g}^{-1}$  (Chen, et al., 2017; C. Y. Wei, et al.,  
148 2018), respectively.

## 149 **2.4. Preparation of SPI-pectin conjugates**

#### 150 **2.4.1. Wet-heating conditions**

151 SPI and pectin (1 : 1 w/w) were dissolved and the pH was adjusted with NaOH  
152 to 6.0, 7.0, 8.0, 9.0, 10.0, 11.0 and 12.0, respectively. The mixed solution was then  
153 reacted at different temperatures (50, 60, 70, 80 and 90 °C) for different times (4, 8, 12,  
154 16, 20 and 24 h). Then, the reactor was immediately cooled in an ice bath for 3 min to  
155 terminate the reaction. The conjugates were freeze-dried and ground into fine powders  
156 for measurements. The optimum pH and temperature were determined by the DG of  
157 the conjugates.

#### 158 **2.4.2. Ultrasound treatment**

159 SPI and pectin (1 : 1 w/w) were mixed at pH 10.0 and 100 mL of the mixtures  
160 were put in a cylinder reactor to be processed with a probe sonicator (JY92-IIDN,  
161 Ningbo Scientz Biotechnology Co., Ningbo, China) with a maximum output power of  
162 900 W and an operating frequency of 22 kHz. The temperature of reactants was  
163 controlled with a water bath and monitored by a temperature probe. Samples were  
164 subjected to ultrasound at different powers (270, 360, 450, 540 and 630 W), durations  
165 (15, 30, 45, 60, 75, 90, 105 and 120 min) and temperatures (50, 60, 70, 80 and 90 °C).  
166 Then, the reactor was immediately cooled in an ice bath for 3 min to terminate the  
167 reaction. The optimum power, duration and temperature were determined by the DG  
168 of the conjugates.

#### 169 **2.5. Measurement of degree of graft (DG)**

170 The DG of conjugates were determined by the modified OPA assay as described  
171 in our previous study (Ma, et al., 2020) and was calculated according to Eqn (1):

172 
$$DG = \frac{A_0 - A_t}{A_0} \times 100\% \quad (1)$$

173 where  $A_0$  is the free amino groups content of the mixtures of SPI and pectin,  $A_t$  is  
174 the free amino groups content of SPI-pectin conjugates prepared with or without  
175 ultrasound.

## 176 **2.6. Sodium-dodecyl-sulfate polyacrylamide gel (SDS-PAGE) electrophoresis**

177 SDS-PAGE electrophoresis was carried out as described in our previous work  
178 (Chen, et al., 2019; Ma, et al., 2020). The stacking gel (5%) and separating gel (12%)  
179 were prepared. Samples, including SPI, SPI and pectin mixtures, and SPI-pectin  
180 conjugates prepared under traditional wet heating or with ultrasound treatment, were  
181 dissolved with a constant protein concentration of  $2 \text{ mg mL}^{-1}$ , and then mixed with the  
182 protein loading dye. The mixtures were heated in boiling water for 5 min and then  
183 loaded in the gel slot. Electrophoresis for the stacking gel and the separating gel was  
184 conducted at 80 V and 120 V, respectively. Gel was stained with Coomassie Brilliant  
185 Blue R250 dye for 30 min followed by destaining in a solution comprising 40%  
186 methanol and 10% acetic acid to the proper color density level.

## 187 **2.7. Measurement of circular dichroism (CD)**

188 Solutions of SPI and SPI-pectin conjugates (prepared under traditional wet  
189 heating or with ultrasound treatment) were prepared at a protein concentration of 0.25  
190  $\text{mg mL}^{-1}$  in the 0.01 M PBS at pH 7.0 and then put in a quartz cuvette of 1 mm optical  
191 path length. The CD spectra of samples were measured by a spectropolarimeter  
192 (JASCO J1500, Tokyo, Japan) at  $20 \text{ }^\circ\text{C} \pm 1 \text{ }^\circ\text{C}$ . Scanning was conducted in the  
193 wavelength range of 190 nm to 250 nm at a rate of  $50 \text{ nm min}^{-1}$  with a bandwidth set

194 at 1 nm. The CD data were expressed in the form of mean residue ellipticity [ $\theta$ ]  
195 (deg cm<sup>2</sup> dmol<sup>-1</sup>). The secondary structures of samples were analyzed using  
196 DICHROWEB.

## 197 **2.8. Measurement of intrinsic fluorescence**

198 Samples were dissolved using 0.01 M PBS solution (pH 7.0) to obtain a protein  
199 concentration of 0.25 mg mL<sup>-1</sup>. The fluorescence spectra ( $\lambda_{\text{ex}}$ , 280 nm;  $\lambda_{\text{em}}$ , 300–500;  
200 slit = 5 nm) were measured with a Model Cary Eclipse spectrophotometer (Varian Inc.,  
201 Palo Alto, USA) at a scanning rate of 600 nm min<sup>-1</sup>.

## 202 **2.9. Measurement of surface hydrophobicity ( $H_0$ )**

203 The  $H_0$  was measured using ANS as a fluorescence probe. Lyophilized samples  
204 were dissolved using 0.01 M PBS solution (pH 7.0) to obtain protein concentrations  
205 ranging from 0.001 mg mL<sup>-1</sup> to 0.4 mg mL<sup>-1</sup>. Then, 50  $\mu$ L of 8 mM ANS was added to  
206 4 mL of sample solutions. Fluorescence intensity ( $\lambda_{\text{ex}}$ , 365 nm;  $\lambda_{\text{em}}$ , 484) was  
207 measured with a Model Cary Eclipse spectrophotometer (Varian Inc., Palo Alto, USA).  
208 The slope of fluorescence intensity versus protein concentration was used as the  $H_0$  of  
209 protein.

## 210 **2.10. Analysis of emulsifying properties**

211 The emulsifying activity index (EAI) and emulsifying stability index (ESI) were  
212 measured according to the method established by Pearce and Kinsella (1978) with  
213 some modifications. Briefly, 5 mL of the blend oil and 15 mL of 2.5 mg mL<sup>-1</sup> samples  
214 were mixed and homogenized at 13500 r for 2 min. The prepared emulsion (50  $\mu$ L)  
215 was then sampled from the bottom of the tube at regular time intervals and diluted

216 with 10 mL of 0.1% (w/v) SDS solution. The absorbance of the diluted emulsion was  
 217 measured at 500 nm. EAI and ESI were calculated by Eqn (2) and (3), respectively:

$$218 \quad \text{EAI (m}^2/\text{g)} = \frac{2 \times 2.303 \times A_0 \times D}{(1-\varphi) \times c \times 10^4} \quad (2)$$

$$219 \quad \text{ESI (\%)} = \frac{A_{10}}{A_0} \times 100\% \quad (3)$$

220 where  $A_0$  and  $A_{10}$  are the absorbance measured at 0 and 10 min, respectively,  $\varphi$  is  
 221 the oil phase fraction,  $c$  is the initial concentration of SPI ( $\text{g mL}^{-1}$ ) and  $D$  is the  
 222 dilution factor.

## 223 **2.11. Statistical analysis**

224 One-way analysis of variance (ANOVA,  $p < 0.05$ ) and Duncan's multiple range  
 225 tests were performed using SPSS 17.0 to evaluate the differences among various  
 226 samples. Data were represented as the means of triple measurements.

## 227 **3. Results and discussion**

### 228 **3.1. Effect of initial pH and temperature on the conjugation of SPI and pectin**

#### 229 **3.1.1. Initial pH**

230 SPI and pectin were conjugated at 70 °C for 24 h at a pH range of 6.0 to 12.0. Fig.  
 231 1 A and B illustrate the DG of the SPI-CP and SPI-AP conjugates, respectively, at  
 232 each tested pH; Fig. 1 C and D show the corresponding appearance of these samples.  
 233 The large molecular weight and complicated structures of both SPI and pectin make it  
 234 difficult for Maillard reaction to take place, leading to the low DG values for all the  
 235 samples as can be observed from Fig. 1 A and B. DG of both conjugates was  
 236 increased as pH was increased from 6.0 to 10.0, possibly attributed to the increased  
 237 proportion of unprotonated amino acid at higher pH (Lertittikul, Benjakul, & Tanaka,

238 2007). However when pH was further increased from 10.0 to 12.0, the DG of both  
239 samples started to decrease, and the solutions turned to a dark brown color (Fig. 1 C  
240 and D). This was considered to be related to the racemization and formation of  
241 lysinoalanine under combined heating-alkaline treatment, which could cause great  
242 damage to SPI (Schwass & Finley, 1984). As well, at an alkaline medium,  
243  $\beta$ -elimination and demethoxylation readily happened inducing pectin molecules to  
244 degrade (Fraeye, et al., 2007), which could also influence the conjugation process. In  
245 this study, the best pH for preparing both samples was determined at pH 10.0.

246 On the other hand, the conjugates prepared by CP can be seen to show an  
247 obviously greater extent of conjugation than AP at each pH. For instance, DG of the  
248 SPI-CP conjugates at pH 10.0 was 20% higher than that of the SPI-AP conjugates,  
249 which was due to the structural differences of the two pectin samples. As can be seen  
250 in Table 1, AP has a significantly higher Mw (1050.50 kDa) than CP (478.00 kDa),  
251 with a larger polydispersity and Rz. The exponent  $\alpha$  from Mark-Houwink equation  
252 ( $[\eta] = KM_w^\alpha$ ) was measured to provide information of pectin chain conformations. As  
253 a characteristic constant,  $\alpha$  indicates the stretching forms of polymers in solution; its  
254 value within the range of 0 – 0.3, 0.5 – 0.8 and 1.0 – 2.0 indicates that polymers are  
255 presented as spheres, flexible chains and rod-like rigid chains, respectively (C. Wei, et  
256 al., 2018). As shown in Table 1,  $\alpha$  for CP and AP was 0.85 and 0.71, respectively,  
257 demonstrating that AP exhibited more flexible chains than CP in the 0.1 mol L<sup>-1</sup>  
258 NaNO<sub>3</sub> solution. These flexible chains can readily intertwine together in the aqueous  
259 system and burry the reactive groups for Maillard reaction, impeding the conjugation

260 process and resulting in the low DG values.

### 261 **3.1.2. Temperature**

262 DG of the SPI-CP and SPI-AP conjugates prepared at different temperatures is  
263 illustrated in Fig. 2 A and B, respectively; the corresponding appearance of these  
264 conjugates is shown in Fig. 2 C and D. Despite the differences in pectin structures,  
265 the optimum temperature for Maillard reaction for both samples was 70 °C, where  
266 the SPI-CP conjugates and SPI-AP conjugates showed the DG values of 8.25% and  
267 6.60%, respectively. This suggested that the variation trend for DG was mainly  
268 influenced by changes in SPI at high temperatures. As reported in previous studies  
269 (Chen, et al., 2019; Mu, et al., 2010), an increase in temperature could accelerate the  
270 Maillard reaction and lead to higher DG of conjugates; however, German,  
271 Damodaran, and Kinsella (1982) have reported that the transition temperature for  
272 glycinin (11s) and  $\beta$ -conglycinin (7s) is 92 °C and 77 °C, respectively, indicating that  
273 there is an “upper threshold”, beyond which the further increase in temperature will  
274 result in severe protein aggregation (Chen, et al., 2019) and in turn, the decreased  
275 DG. Looking at Fig. 2 C and D, both conjugates formed at 90 °C presented a deep  
276 brown color and precipitated a lot after being placed for a few minutes (not shown in  
277 pictures). Mu, et al. (2010) has reported that high temperatures could induce serious  
278 browning of conjugates, while the phase separation can be attributed to the insoluble  
279 protein aggregates formed at high temperatures as mentioned above.

## 280 **3.2. Effect of ultrasound conditions on the conjugation of SPI and pectin**

### 281 **3.2.1. Ultrasound power**



282 DG of SPI-pectin conjugates prepared at different ultrasound powers for 20 min  
283 is depicted in Fig. 3. As ultrasound power was increased from 270 W to 450 W, DG  
284 of SPI-CP and SPI-AP conjugates was significantly increased by 248.43% and  
285 85.63%, respectively, indicating that more energy input accelerated the Maillard  
286 reaction and led to a higher grafting extent. This was in line with the previous  
287 observations (Chen, et al., 2019; Li, et al., 2014; Mu, et al., 2010). Li, et al. (2014)  
288 applied ultrasound to the Maillard reaction of PPI and glucomannan; it was found  
289 that when the ultrasound intensity was increased from 302.55 W cm<sup>-2</sup> to 786.62 W  
290 cm<sup>-2</sup> at 60 °C, 70 °C and 80 °C, the DG of PPI-glucomannan conjugates was  
291 increased by 90.66%, 55.25% and 65.84%, respectively. High-intensity ultrasound is  
292 able to induce local translational motions and strong micro-jets in liquid systems,  
293 which bring reactive groups into closer proximity and enhance their contacts,  
294 resulting in a more steady grafting process (Chen, et al., 2016). Furthermore, it has  
295 also been suggested that proper doses of ultrasound could generate certain amounts  
296 of shear forces and free radicals that favorably modify the structures of proteins and  
297 polysaccharides, causing more exposure of amino and carbonyl radicals for Maillard  
298 reaction (Chen, et al., 2016; Qu, et al., 2018). However, looking at Fig. 3, when the  
299 ultrasound power was further increased beyond 450 W, the DG of both conjugates  
300 started to decrease, indicating that after exceeding a certain level of energy input,  
301 proteins would be denatured by the shear forces and free radicals produced from the  
302 intense ultrasonic field, leading to the formation of protein aggregates and thus  
303 impeding the grafting process (Chen, et al., 2019; Resendiz-Vazquez, et al., 2017).

304 Similar phenomenon was also observed in our previous study (Chen, et al., 2019),  
305 where the DG of whey protein isolate (WPI)-gum acacia (GA) conjugates was firstly  
306 increased as the ultrasonic power was increased from 100 W to 500 W, whereas it  
307 decreased as the power was further increased to 700 W.

### 308 **3.2.2. Temperature**

309 The DG of SPI-pectin conjugates prepared at different temperatures under an  
310 ultrasonic field at 450 W for 20 min is depicted in Fig. 4. Similar to the routine  
311 wet-heating process, DG of SPI-CP and SPI-AP conjugates was observed to increase  
312 from 3.76% to 8.25%, and 2.93% to 6.60%, respectively, when the temperature was  
313 increased from 50 °C to 70 °C; whereas it was decreased to 3.57% and 0.27%,  
314 respectively for CP and AP, as the temperature was further increased to 90 °C. Qu, et  
315 al. (2018) has reported that ultrasound treatment could increase the optimum  
316 temperature for conjugation of RPI and dextran. Authors ascribed this to the  
317 ultrasound cavitation increasing the denaturation temperature of RPI and thus  
318 preventing protein aggregations at high temperatures. However in this study, DG of  
319 both conjugates prepared with and without ultrasound treatment peaked at 70 °C,  
320 indicating that at 80 °C and 90 °C, the effect of thermal denaturation of SPI might  
321 outweigh the positive effects brought by ultrasound irradiation.

### 322 **3.2.3. Ultrasound duration**

323 The DG of SPI-CP/AP conjugates prepared by traditional wet heating and  
324 ultrasound treatment at different times is shown in Table 2. Ultrasound treatment at  
325 short bursts of time can be seen to significantly accelerate the Maillard reaction

326 between SPI and pectin. For example, the DG of SPI-CP conjugates treated by  
327 ultrasound at 45 min was 24.06%, nearly treble the value obtained by wet heating for  
328 24 h. As stated before, the favorable changes in structures of both macromolecules,  
329 as well as the enhanced contacts of the reactants under a high-intensity ultrasonic  
330 field could result in an improved grafting process. Similar observations have been  
331 reported for WPI-GA (Chen, et al., 2019), SPI-GA (Mu, et al., 2010) and  
332 PPI-glucomannan conjugates (Li, et al., 2014) prepared with ultrasound treatment.  
333 However, prolonged ultrasound irradiation was observed to be less beneficial for the  
334 grafting process. As shown in Table 2, when ultrasound duration was increased from  
335 15 min to 45 min, the DG of SPI-CP conjugates was increased by 128.71%; whereas  
336 when the duration was further prolonged to 120 min, the increase in DG can be seen  
337 to hit the plateau and was only 10.85%. Similarly, when ultrasound was applied to  
338 the conjugation between SPI and AP, the DG of SPI-AP conjugates treated at a  
339 duration of 60 min was 261.44% higher than that at 15 min; while for the last 60 min  
340 (from 60 min to 120 min), the DG was increased by only 14.66%. These results  
341 suggested that long-time ultrasound treatment might denature the proteins (Zhu, et  
342 al., 2018) and lead to a decreased grafting efficiency. Considering both productivity  
343 and energy efficiency, the ultrasound durations for the preparation of the SPI-CP and  
344 SPI-AP conjugates were selected at 45 min and 60 min, respectively.

345 It is also worthwhile to note that the increase in the DG of SPI-AP conjugates  
346 with ultrasound treatment was higher than that of the SPI-CP conjugates. Table 1  
347 lists the conformational parameters of CP and AP with and without ultrasound

348 treatment. After being treated with ultrasound for a certain duration, both pectin  
349 samples showed significantly lower Mw and Rz, and their polysaccharide chains  
350 tended to be more rigid (with an increased exponent  $\alpha$ ), which in combination  
351 facilitated the conjugation process with SPI. Ultrasound mechanical breakage is  
352 known to act on the midpoint of polymer chains (Koda, Taguchi, & Futamura, 2011)  
353 and is more effective for long-chain polymers (Portenlanger, et al., 1997). Therefore,  
354 AP with higher Mw was more accessible for ultrasound breakage, resulting in a  
355 larger increase in the grafting extent than CP. Furthermore, under a high-intensity  
356 ultrasonic field, CP would be degraded into small segments at a shorter treatment  
357 time compared to AP, making ultrasound less effective for degradation. This also  
358 explained why the optimum condition for SPI-CP conjugation was obtained at a  
359 shorter ultrasound duration.

#### 360 **3.2.4. SDS-PAGE analysis**

361 Fig. 5 shows the SDS-PAGE profiles of SPI, mixtures of SPI and pectin samples,  
362 and SPI-pectin conjugates prepared by wet heating and ultrasound treatment. SPI  
363 mainly consists of glycinin (11s globulin) and  $\beta$ -conglycinin (7s globulin), which are  
364 known to contain a series of polypeptide chains with diverse Mw (Petruccelli & Anon,  
365 1995). The two mixture samples in Lanes 2 and 3 showed a same pattern as the native  
366 SPI, indicating that both pectin samples contained little protein impurities and did not  
367 change the electrophoretic profiles of SPI. However, the Maillard reaction generated  
368 various conjugated products with too large Mw, which can be seen to form a new  
369 band on the top of the separating gel in Lanes 4 to 7. Meanwhile, compared with

370 Lanes 1–3, the featured bands of SPI at the Mw range of 15 kDa, 25–35 kDa and 55–  
371 70 kDa clearly faded out in Lanes 4–7, indicating that these proteins had participated  
372 in the grafting process. Furthermore, compared with the conjugated samples prepared  
373 by the traditional wet heating, the ultrasound-treated conjugates displayed darker new  
374 bands and lighter featured bands of the native SPI, indicating the greater grafting  
375 extent for these samples, which is in line with the results of DG analysis.

### 376 **3.2.5. CD analysis**

377 The far-UV CD spectrum was employed to identify the variations in the  
378 secondary structures of SPI during different conjugation processes. Fig. 6 depicts the  
379 CD spectra of SPI, mixtures of SPI and pectin samples and SPI-pectin conjugates  
380 prepared by wet heating and ultrasound treatment, and Table 3 summarizes the  
381 secondary structures of each sample. Huang, Ding, Dai, and Ma (2017) analyzed the  
382 secondary structures of SPI and found that the contents of  $\alpha$ -helix,  $\beta$ -sheet, turn and  
383 random coil were 6.5%, 36.7%, 23.0% and 33.8%, respectively, which is very similar  
384 to our results. As shown in Table 3, the simple physical mixing with pectin samples  
385 did not change the secondary structures of SPI. However, the conjugation process by  
386 either traditional wet heating or ultrasound treatment reduced the contents of  $\alpha$ -helix,  
387  $\beta$ -sheet and turn in the protein conformation, whereas it increased the contents of the  
388 random coil. Similar results were reported by Mu, et al. (2010), where the contents of  
389  $\alpha$ -helix,  $\beta$ -sheet and turn in the SPI-GA conjugates were decreased by 73.58%, 76.69%  
390 and 46.79%, respectively, while the contents of the random coil were increased by  
391 112.95%, compared to the original SPI. It has been reported that the  $\alpha$ -helix and

392  $\beta$ -sheet are generally buried inside the polypeptide chains (Mu, et al., 2010), therefore  
393 the decrease of these structures indicated that the attachment of CP or AP changed the  
394 spatial conformation of SPI and led to a looser protein structure (Qu, et al., 2018). The  
395 increase in the content of random coil further confirmed the unfolding of proteins  
396 during the Maillard reaction resulting in a more disordered molecular structure.  
397 However, the SPI-CP and SPI-AP conjugates prepared by the same conjugation  
398 process (*i.e.* traditional wet heating or ultrasound treatment) showed similar secondary  
399 structures, indicating that the grafting method rather than the different pectin samples  
400 played a more important role in changing the secondary structures of proteins. It was  
401 revealed that the conjugates prepared by ultrasound treatment lost more  $\alpha$ -helix and  
402  $\beta$ -sheet but gained more random coil compared to those obtained by traditional wet  
403 heating, suggesting that in addition to the grafting process, ultrasound also had a hand  
404 in breaking the peptide bonds and unfolding the proteins, which was reported to be  
405 related to the pressure alterations and turbulence generated from cavitation (Mu, et al.,  
406 2010). Such an extension in the protein structures possibly made SPI more favorable  
407 for binding to pectin, which could be a reason for the higher DG values obtained  
408 under an ultrasonic field as described in Section 3.2.3. These structural  
409 transformations led to a greater conformational flexibility of proteins, allowing for  
410 easier adsorption at the oil-water interface and could result in the improved  
411 emulsifying properties (Martínez, Sanchez, Ruíz-Henestrosa, Patino, & Pilosof,  
412 2007).

### 413 **3.2.6. Intrinsic fluorescence analysis**

414 Alterations in the proteins' tertiary structures during conjugation were  
415 determined by the intrinsic fluorescence spectra based on the tryptophan (Trp) content.  
416 Fig. 7 depicts the intrinsic fluorescence spectra of SPI, mixtures of SPI and pectin  
417 samples and SPI-pectin conjugates prepared with and without ultrasound treatment. It  
418 was shown that the highest fluorescence intensity of the original SPI was obtained at  
419 341 nm; and this maximum absorption wavelength ( $\lambda_{\max}$ ) remained unchanged for the  
420 two mixture samples. However, a slight decrease in the intensity can be observed for  
421 both mixtures, as a result of the steric-hindrance effect of pectin samples. As  
422 mentioned in Section 3.1.1, AP had a higher Mw and more flexible chains than CP, so  
423 it could induce a stronger steric-hindrance effect and in turn, a lower fluorescence  
424 intensity. Conjugation under the traditional wet heating conditions caused a further  
425 decrease in the fluorescence intensity, and it led the  $\lambda_{\max}$  to shift from 341 nm to 343  
426 nm, suggesting that the Trp residues reached a more exposed and polar  
427 microenvironment (Sheng, et al., 2020). The transformation of SPI secondary  
428 structures, exposure of hydrophobic groups in proteins, and the shielding effects of  
429 pectin during the Maillard reaction were considered as the reasons for this  
430 phenomenon (Sheng, et al., 2017; Sheng, et al., 2020). As the DG of both conjugates  
431 were very low (as shown in Table 2), the steric-hindrance effect of pectin still played a  
432 main role in shielding the fluorescence signals and thus the SPI-AP conjugates  
433 showed a lower fluorescence intensity than the SPI-CP conjugates. Compared to the  
434 conjugates obtained by traditional wet heating, the conjugates prepared with  
435 ultrasound can be seen to have much less compact tertiary structures, with

436 significantly lower fluorescence intensities and a greater red shift to 345 nm. This was  
437 possibly due to the unfolding of protein molecules and the destroyed hydrophobic  
438 interactions during ultrasound treatment (Subhedar & Gogate, 2014). Despite the  
439 more complex structures and the potentially stronger shielding effect of AP, the  
440 ultrasound-treated SPI-CP conjugates showed an overall lower fluorescence intensity  
441 than the SPI-AP conjugates, which can be ascribed to the greater grafting extent.

### 442 **3.2.7. $H_0$ analysis**

443  $H_0$  is one of the most important factors determining a range of functional  
444 properties of proteins, such as the solubility, emulsifying ability and foaming ability  
445 (Jiang, et al., 2015). Here we employed a hydrophobic fluorescent dye, *i.e.* ANS, to  
446 evaluate the  $H_0$  of SPI, SPI and pectin mixtures, and SPI-CP/AP conjugates prepared  
447 by wet heating and ultrasound treatment; results are shown in Fig. 8. The addition of  
448 CP or AP can be seen to block the way of ANS to the hydrophobic residues, resulting  
449 in the 38.93% and 40.08% lower  $H_0$  values for the SPI-CP and SPI-AP mixtures,  
450 respectively, compared to the original SPI. Glycosylation under the traditional wet  
451 heating conditions induced further reduction in the  $H_0$ , indicating that the Maillard  
452 reaction has changed the SPI conformation and restrained the exposure of  
453 hydrophobic groups (Sheng, et al., 2020); also, it might have produced advanced  
454 glycation products with little surface hydrophobicity (Chen, et al., 2016). When  
455 ultrasound was introduced to the conjugation process, a significant increase in  $H_0$  can  
456 be observed for both conjugates, which was in accord with the previous studies (Chen,  
457 et al., 2016; Li, et al., 2014). This can be attributed to the unfolding of proteins and/or



458 dissociation of protein aggregates under a high-intensity ultrasonic field, leading to  
459 the exposure of the previously buried hydrophobic groups (Chen, et al., 2016). The  
460 increased  $H_0$  is known to be able to increase proteins' adsorption rate to the oil/water  
461 interface, which is helpful in improving the emulsifying properties (Delahaije,  
462 Gruppen, Giuseppin, & Wierenga, 2014). Furthermore, despite the higher DG of the  
463 SPI-CP conjugates, no significant differences were observed for  $H_0$  of the SPI-CP and  
464 SPI-AP conjugates under a specific conjugation condition (*i.e.* wet heating or  
465 ultrasound treatment), which was possibly due to the stronger steric-hindrance effect  
466 provided by AP.

#### 467 **3.2.8. Emulsifying properties analysis**

468 Fig. 9 shows the EAI and ESI of SPI, SPI and pectin mixtures, and SPI-CP/AP  
469 conjugates prepared by wet heating and ultrasound treatment. Both indices were  
470 increased with the addition of CP or AP, possibly due to the emulsifying properties  
471 provided by pectin samples. It has been recognized that the conjugation of protein and  
472 polysaccharide combines the characteristic property of proteins to adsorb strongly to  
473 the oil-water interface, with the excellent solubility of polysaccharides in the aqueous  
474 medium (Dickinson & Galazka, 1991). As expected, conjugation under the traditional  
475 wet heating conditions significantly improved the emulsifying properties of the  
476 SPI-CP/AP conjugates when compared to the original SPI; however, due to the low  
477 DG of both conjugates (less than 10%), there were no significant differences in EAI  
478 and ESI as compared with the mixture samples. Nevertheless, ultrasound can be seen  
479 to significantly improve the emulsifying properties of both conjugates. As shown in

480 Fig. 9, the EAI and ESI of the ultrasound-treated SPI-CP conjugates were increased  
481 by 147.59% and 102.76%, respectively, compared to those prepared by the traditional  
482 wet heating; as for the SPI-AP conjugates, the EAI and ESI were significantly  
483 increased by 104.42% and 111.56%, respectively, compared to those prepared by the  
484 traditional wet heating. As described in the above sections, the improved DG,  
485 enhanced surface hydrophobicity, together with the extended spatial conformations of  
486 proteins obtained with ultrasound treatment, have contributed to this significant  
487 enhancement in the emulsifying properties of the conjugates. As can be seen, the  
488 SPI-CP/AP conjugates prepared by ultrasound demonstrated satisfying emulsifying  
489 properties (with the EAI more than 30% and ESI more than 80%), suggesting that  
490 both pectin samples in conjugation with SPI can form excellent emulsions under a  
491 high-intensity ultrasonic field.

#### 492 **4. Conclusions**

493 In this work, SPI was conjugated with CP and AP via traditional wet heating or  
494 ultrasound treatment. Ultrasound treatment at a power of 450 W and a temperature of  
495 70 °C significantly accelerated the conjugation processes between SPI and pectin  
496 samples and led to much greater grafting extents compared to the traditional wet  
497 heating. However, it took a longer time for SPI-AP conjugates to achieve a desirable  
498 DG when compared to the SPI-CP conjugates, possibly attributed to the larger  
499 molecular weight and the more flexible structure of AP. Considering both productivity  
500 and energy efficiency, the ultrasound durations for preparing the SPI-CP and SPI-AP  
501 conjugates were selected at 45 min and 60 min, achieving the DG of 24.06% and

502 20.06%, respectively. SDS-PAGE analysis confirmed that the conjugates were formed  
503 between SPI and pectin samples. CD spectra showed that the ultrasound-assisted  
504 conjugation process led to lower contents of  $\alpha$ -helix and  $\beta$ -sheet, and higher contents  
505 of random coil. Fluorescence spectra showed that the conjugates prepared with  
506 ultrasound had much less compact tertiary structures, with lower fluorescence  
507 intensities and a greater red shift. These results suggested that in addition to the  
508 grafting process, ultrasound also played a marked role in the unfolding of SPI,  
509 resulting in more favorable structures for Maillard reaction. Furthermore, the  
510 application of ultrasound to the conjugation process significantly increased the  
511 hydrophobicity and emulsifying properties of both conjugates. Despite the different  
512 structures of CP and AP and their different performance in conjugation with SPI, no  
513 significant differences were observed for the emulsifying properties of the two  
514 conjugates, indicating that both pectin samples were capable of forming excellent  
515 conjugates with ultrasound treatment.

#### 516 **Declarations of interest**

517 None.

#### 518 **Acknowledgement**

519 This work was financially supported by the National Natural Science Foundation  
520 of China (31901822), China Postdoctoral Science Foundation (2017M620247),  
521 International Postdoctoral Exchange Fellowship Program (20180083), the National  
522 Key Research and Development Program of China (2016YFD0400301) and Primary

523 Research and Development Plan of Zhejiang Province, China (2015C02036).

524 **References**

- 525 Bouyer, E., Mekhloufi, G., Rosilio, V., Grossiord, J.-L., & Agnely, F. (2012). Proteins,  
526 polysaccharides, and their complexes used as stabilizers for emulsions:  
527 alternatives to synthetic surfactants in the pharmaceutical field? *International*  
528 *Journal of Pharmaceutics*, *436* (1-2), 359-378.
- 529 Chan, S. Y., Choo, W. S., Young, D. J., & Loh, X. J. (2017). Pectin as a rheology  
530 modifier: Origin, structure, commercial production and rheology. *Carbohydrate*  
531 *Polymers*, *161*, 118-139.
- 532 Chen, J. L., Cheng, H., Wu, D., Linhardt, R. J., Zhi, Z. J., Yan, L. F., Chen, S. G., &  
533 Ye, X. Q. (2017). Green recovery of pectic polysaccharides from citrus canning  
534 processing water. *Journal of Cleaner Production*, *144*, 459-469.
- 535 Chen, L., Chen, J., Wu, K., & Yu, L. (2016). Improved low pH emulsification  
536 properties of glycated peanut protein isolate by ultrasound Maillard reaction.  
537 *Journal of Agricultural and Food Chemistry*, *64* (27), 5531-5538.
- 538 Chen, W., Ma, X., Wang, W., Lv, R., Guo, M., Ding, T., Ye, X., Miao, S., & Liu, D.  
539 (2019). Preparation of modified whey protein isolate with gum acacia by  
540 ultrasound Maillard reaction. *Food Hydrocolloids*, *95*, 298-307.
- 541 de Oliveira, F. C., Coimbra, J. S. d. R., de Oliveira, E. B., Zuñiga, A. D. G., & Rojas,  
542 E. E. G. (2016). Food protein-polysaccharide conjugates obtained via the  
543 Maillard reaction: A review. *Critical Reviews in Food Science and Nutrition*, *56*  
544 (7), 1108-1125.

- 545 Delahaije, R. J., Gruppen, H., Giuseppin, M. L., & Wierenga, P. A. (2014).  
546 Quantitative description of the parameters affecting the adsorption behaviour of  
547 globular proteins. *Colloids and surfaces B: Biointerfaces*, *123*, 199-206.
- 548 Dickinson, E., & Galazka, V. B. (1991). Emulsion stabilization by ionic and covalent  
549 complexes of  $\beta$ -lactoglobulin with polysaccharides. *Food Hydrocolloids*, *5* (3),  
550 281-296.
- 551 Fraeye, I., De Roeck, A., Duvetter, T., Verlent, I., Hendrickx, M., & Van Loey, A.  
552 (2007). Influence of pectin properties and processing conditions on thermal pectin  
553 degradation. *Food Chemistry*, *105* (2), 555-563.
- 554 German, B., Damodaran, S., & Kinsella, J. E. (1982). Thermal dissociation and  
555 association behavior of soy proteins. *Journal of Agricultural and Food Chemistry*,  
556 *30* (5), 807-811.
- 557 Guan, Y. G., Lin, H., Han, Z., Wang, J., Yu, S. J., Zeng, X. A., Liu, Y. Y., Xu, C. H., &  
558 Sun, W. W. (2010). Effects of pulsed electric field treatment on a bovine serum  
559 albumin–dextran model system, a means of promoting the Maillard reaction.  
560 *Food Chemistry*, *123* (2), 275-280.
- 561 Huang, L., Ding, X., Dai, C., & Ma, H. (2017). Changes in the structure and  
562 dissociation of soybean protein isolate induced by ultrasound-assisted acid  
563 pretreatment. *Food Chemistry*, *232*, 727-732.
- 564 Jiang, L., Wang, Z., Li, Y., Meng, X., Sui, X., Qi, B., & Zhou, L. (2015). Relationship  
565 between surface hydrophobicity and structure of soy protein isolate subjected to  
566 different ionic strength. *International Journal of Food Properties*, *18* (5),

- 567 1059-1074.
- 568 Koda, S., Taguchi, K., & Futamura, K. (2011). Effects of frequency and a radical  
569 scavenger on ultrasonic degradation of water-soluble polymers. *Ultrasonics*  
570 *Sonochemistry*, 18 (1), 276-281.
- 571 Lertittikul, W., Benjakul, S., & Tanaka, M. (2007). Characteristics and antioxidative  
572 activity of Maillard reaction products from a porcine plasma protein–glucose  
573 model system as influenced by pH. *Food Chemistry*, 100 (2), 669-677.
- 574 Li, C., Huang, X., Peng, Q., Shan, Y., & Xue, F. (2014). Physicochemical properties  
575 of peanut protein isolate–glucomannan conjugates prepared by ultrasonic  
576 treatment. *Ultrasonics Sonochemistry*, 21 (5), 1722-1727.
- 577 Ma, X., Chen, W., Yan, T., Wang, D., Hou, F., Miao, S., & Liu, D. (2020).  
578 Comparison of citrus pectin and apple pectin in conjugation with soy protein  
579 isolate (SPI) under controlled dry-heating conditions. *Food Chemistry*, 309,  
580 125501.
- 581 Ma, X., Yan, T., Hou, F., Chen, W., Miao, S., & Liu, D. (2019). Formation of soy  
582 protein isolate (SPI)-citrus pectin (CP) electrostatic complexes under a  
583 high-intensity ultrasonic field: Linking the enhanced emulsifying properties to  
584 physicochemical and structural properties. *Ultrasonics Sonochemistry*, 59,  
585 104748.
- 586 Martínez, K. D., Sanchez, C. C., Ruíz-Henestrosa, V. P., Patino, J. M. R., & Pilosof, A.  
587 M. (2007). Effect of limited hydrolysis of soy protein on the interactions with  
588 polysaccharides at the air–water interface. *Food Hydrocolloids*, 21 (5-6),

- 589 813-822.
- 590 Mu, L., Zhao, M., Yang, B., Zhao, H., Cui, C., & Zhao, Q. (2010). Effect of ultrasonic  
591 treatment on the graft reaction between soy protein isolate and gum acacia and on  
592 the physicochemical properties of conjugates. *Journal of Agricultural and Food  
593 Chemistry*, 58 (7), 4494-4499.
- 594 Nooshkam, M., & Varidi, M. (2019). Maillard conjugate-based delivery systems for  
595 the encapsulation, protection, and controlled release of nutraceuticals and food  
596 bioactive ingredients: A review. *Food Hydrocolloids*, 105389.
- 597 Pearce, K. N., & Kinsella, J. E. (1978). Emulsifying properties of proteins: evaluation  
598 of a turbidimetric technique. *Journal of Agricultural and Food Chemistry*, 26 (3),  
599 716-723.
- 600 Petruccelli, S., & Anon, M. C. (1995). Soy protein isolate components and their  
601 interactions. *Journal of Agricultural and Food Chemistry*, 43 (7), 1762-1767.
- 602 Portenlanger, G., Heusinger, H., Coimbra, M. A., Barros, A., Barros, M., Rutledge, D.  
603 N., & Delgadillo, I. (1997). The influence of frequency on the mechanical and  
604 radical effects for the ultrasonic degradation of dextrans. *Ultrasonics  
605 Sonochemistry*, 4 (2), 127-130.
- 606 Qu, W., Zhang, X., Chen, W., Wang, Z., He, R., & Ma, H. (2018). Effects of ultrasonic  
607 and graft treatments on grafting degree, structure, functionality, and digestibility  
608 of rapeseed protein isolate-dextran conjugates. *Ultrasonics Sonochemistry*, 42,  
609 250-259.
- 610 Resendiz-Vazquez, J., Ulloa, J., Urías-Silvas, J., Bautista-Rosales, P.,

- 611        Ramírez-Ramírez, J., Rosas-Ulloa, P., & González-Torres, L. (2017). Effect of  
612        high-intensity ultrasound on the technofunctional properties and structure of  
613        jackfruit (*Artocarpus heterophyllus*) seed protein isolate. *Ultrasonics*  
614        *Sonochemistry*, 37, 436-444.
- 615        Schwass, D. E., & Finley, J. W. (1984). Heat and alkaline damage to proteins:  
616        racemization and lysinoalanine formation. *Journal of Agricultural and Food*  
617        *Chemistry*, 32 (6), 1377-1382.
- 618        Sheng, L., Su, P., Han, K., Chen, J., Cao, A., Zhang, Z., Jin, Y., & Ma, M. (2017).  
619        Synthesis and structural characterization of lysozyme–pullulan conjugates  
620        obtained by the Maillard reaction. *Food Hydrocolloids*, 71, 1-7.
- 621        Sheng, L., Tang, G., Wang, Q., Zou, J., Ma, M., & Huang, X. (2020). Molecular  
622        characteristics and foaming properties of ovalbumin-pullulan conjugates through  
623        the Maillard reaction. *Food Hydrocolloids*, 100, 105384.
- 624        Silván, J. M., Assar, S. H., Srey, C., Del Castillo, M. D., & Ames, J. M. (2011).  
625        Control of the Maillard reaction by ferulic acid. *Food Chemistry*, 128 (1),  
626        208-213.
- 627        Subhedar, P. B., & Gogate, P. R. (2014). Enhancing the activity of cellulase enzyme  
628        using ultrasonic irradiations. *Journal of Molecular Catalysis B: Enzymatic*, 101,  
629        108-114.
- 630        Wang, X. S., Tang, C. H., Li, B. S., Yang, X. Q., Li, L., & Ma, C. Y. (2008). Effects of  
631        high-pressure treatment on some physicochemical and functional properties of  
632        soy protein isolates. *Food Hydrocolloids*, 22 (4), 560-567.



- 633 Wei, C., He, P., He, L., Ye, X., Cheng, J., Wang, Y., Li, W., & Liu, Y. (2018). Structure  
634 characterization and biological activities of a pectic polysaccharide from cupule  
635 of *Castanea henryi*. *International Journal of Biological Macromolecules*, *109*,  
636 65-75.
- 637 Wei, C. Y., He, P. F., He, L., Ye, X. Q., Cheng, J. W., Wang, Y. B., Li, W. Q., & Liu, Y.  
638 (2018). Structure characterization and biological activities of a pectic  
639 polysaccharide from cupule of *Castanea henryi*. *International Journal of*  
640 *Biological Macromolecules*, *109*, 65-75.
- 641 Xu, C. H., Yu, S. J., Yang, X. Q., Qi, J. R., Lin, H., & Zhao, Z. G. (2010). Emulsifying  
642 properties and structural characteristics of  $\beta$  - conglycinin and dextran  
643 conjugates synthesised in a pressurised liquid system. *International Journal of*  
644 *Food Science & Technology*, *45* (5), 995-1001.
- 645 Yang, Y., Cui, S., Gong, J., Miller, S. S., Wang, Q., & Hua, Y. (2015). Stability of  
646 citral in oil-in-water emulsions protected by a soy protein-polysaccharide  
647 Maillard reaction product. *Food Research International*, *69*, 357-363.
- 648 Yu, H., Seow, Y.-X., Ong, P. K., & Zhou, W. (2017). Effects of high-intensity  
649 ultrasound on Maillard reaction in a model system of d-xylose and l-lysine.  
650 *Ultrasonics Sonochemistry*, *34*, 154-163.
- 651 Zhang, Q., Li, L., Lan, Q., Li, M., Wu, D., Chen, H., Liu, Y., Lin, D., Qin, W., &  
652 Zhang, Z. (2019). Protein glycosylation: a promising way to modify the  
653 functional properties and extend the application in food system. *Critical Reviews*  
654 *in Food Science and Nutrition*, *59* (15), 2506-2533.

655 Zhu, Z., Zhu, W., Yi, J., Liu, N., Cao, Y., Lu, J., Decker, E. A., & McClements, D. J.

656 (2018). Effects of sonication on the physicochemical and functional properties of

657 walnut protein isolate. *Food Research International*, 106, 853-861.

658

Journal Pre-proof

## Figure captions

**Fig. 1** Effects of pH on the DG of (A) SPI-CP conjugates (70 °C, 24 h) and (B) SPI-AP conjugates (70 °C, 24 h); and the morphology of (C) SPI-CP conjugates and (D) SPI-AP conjugates.

**Fig. 2** Effects of temperature on the DG of (A) SPI-CP conjugates (pH 10.0, 24 h) and (B) SPI-AP conjugates (pH 10.0, 24 h); and the morphology of (C) SPI-CP conjugates and (D) SPI-AP conjugates.

**Fig. 3** Effects of ultrasound power on the DG of SPI-pectin conjugates (pH 10.0, 70 °C, 20 min).

**Fig. 4** Effects of ultrasound temperature on the DG of SPI-pectin conjugates (450 W, pH 10.0, 20 min).

**Fig. 5** SDS-PAGE of SPI, mixtures of SPI and pectin, and SPI-pectin conjugates prepared by traditional wet heating and ultrasound treatment. Lane M, molecular weight markers (kDa); Lane 1, SPI; Lane 2, mixtures of SPI and CP; Lane 3, mixtures of SPI and AP; Lane 4, SPI-CP conjugates prepared by traditional wet heating (70 °C, 24 h); Lane 5, SPI-AP conjugates prepared by traditional wet heating (70 °C, 24 h); Lane 6, SPI-CP conjugates prepared with ultrasound treatment (450 W, 70 °C, 45 min); Lane 7, SPI-AP conjugates prepared with ultrasound treatment (450 W, 70 °C, 60 min).

**Fig. 6** CD spectra of SPI, mixtures of SPI and pectin, and SPI-pectin conjugates prepared by traditional wet heating (70 °C, 24 h) and ultrasound treatment (450 W, 70 °C; 45 min for the SPI-CP conjugates and 60 min for the SPI-AP conjugates).

**Fig. 7** Intrinsic fluorescence spectra of SPI, mixtures of SPI and pectin, and SPI-pectin conjugates prepared by traditional wet heating (70 °C, 24 h) and

ultrasound treatment (450 W, 70 °C; 45 min for the SPI-CP conjugates and 60 min for the SPI-AP conjugates).

**Fig. 8**  $H_0$  of SPI, mixtures of SPI and pectin, and SPI-pectin conjugates prepared by traditional wet heating (70 °C, 24 h) and ultrasound treatment (450 W, 70 °C; 45 min for the SPI-CP conjugates and 60 min for the SPI-AP conjugates).

**Fig. 9** The EAI and ESI of SPI, mixtures of SPI and pectin, and SPI-pectin conjugates prepared by traditional wet heating (70 °C, 24 h) and ultrasound treatment (450 W, 70 °C; 45 min for the SPI-CP conjugates and 60 min for the SPI-AP conjugates).

## Tables

**Table 1** Conformational parameters of pectin samples with and without ultrasound treatment (450 W, 70 °C).

Parameters	CP	CP	AP	AP
		(with ultrasound for 45 min)		(with ultrasound for 60 min)
$M_w$ (kDa)	$478.00 \pm 0.60^c$	$246.40 \pm 1.80^d$	$1050.50 \pm 5.50^a$	$575.50 \pm 0.80^b$
$M_n$ (kDa)	$188.00 \pm 0.10^c$	$115.60 \pm 1.50^d$	$314.10 \pm 1.10^a$	$249.00 \pm 4.30^b$
Polydispersity	$2.54 \pm 0.00^b$	$2.13 \pm 0.04^d$	$3.34 \pm 0.03^a$	$2.31 \pm 0.04^c$
$R_z$ (nm)	$36.80 \pm 0.00^{b,c}$	$34.60 \pm 0.20^c$	$40.70 \pm 0.50^a$	$38.00 \pm 1.20^b$
$\alpha$	$0.84 \pm 0.00^b$	$0.89 \pm 0.01^a$	$0.71 \pm 0.03^d$	$0.79 \pm 0.00^c$

*Note:* values with different italic superscript letters (a–d) in the same column within each pectin indicate significant differences as estimated by Duncan's multiple range test ( $P < 0.05$ ).

**Table 2** The DG of SPI-CP/AP conjugates prepared by wet heating and ultrasound treatment (450 W) at pH 10.0 and 70 °C.

Samples	Wet heating		With ultrasound	
	Time (h)	DG (%)	Time (min)	DG (%)
SPI-CP conjugates	4	1.92 ± 0.09 <sup>f</sup>	15	10.52 ± 0.57 <sup>f</sup>
	8	2.75 ± 0.18 <sup>e</sup>	30	17.29 ± 0.16 <sup>e</sup>
	12	3.85 ± 0.37 <sup>d</sup>	45	24.06 ± 0.08 <sup>d</sup>
	16	5.96 ± 0.27 <sup>c</sup>	60	24.55 ± 0.41 <sup>c,d</sup>
	20	6.78 ± 0.00 <sup>b</sup>	75	25.12 ± 0.16 <sup>c,d</sup>
	24	8.25 ± 0.18 <sup>a</sup>	90	25.53 ± 0.57 <sup>b,c</sup>
			105	26.51 ± 0.08 <sup>a,b</sup>
		120	26.67 ± 0.08 <sup>a</sup>	
SPI-AP conjugates	4	1.92 ± 0.64 <sup>c</sup>	15	5.55 ± 0.49 <sup>f</sup>
	8	3.12 ± 0.18 <sup>c</sup>	30	11.74 ± 0.33 <sup>e</sup>
	12	4.58 ± 0.37 <sup>b</sup>	45	16.64 ± 0.33 <sup>d</sup>
	16	5.13 ± 0.18 <sup>b</sup>	60	20.06 ± 0.49 <sup>c</sup>
	20	5.50 ± 0.37 <sup>a,b</sup>	75	20.55 ± 0.16 <sup>b,c</sup>
	24	6.60 ± 0.37 <sup>a</sup>	90	21.37 ± 0.49 <sup>b</sup>
			105	22.76 ± 0.24 <sup>a</sup>
		120	23.00 ± 0.16 <sup>a</sup>	

Note: values with different italic superscript letters (a–d) in the same column within each conjugate sample indicate significant differences as estimated by Duncan's multiple range test ( $P < 0.05$ ).

**Table 3** Secondary structures of SPI, mixtures of SPI and pectin samples, and SPI-pectin conjugates prepared by traditional wet heating (70 °C, 24 h) and ultrasound treatments (450 W, 70 °C; 45 min for the SPI-CP conjugates and 60 min for the SPI-AP conjugates).

	$\alpha$ -Helix (%)	$\beta$ -Sheet (%)	Turn (%)	Random coil (%)
SPI	6.70	38.30	22.10	32.90
Mixtures of SPI and CP	6.70	38.30	22.10	32.90
Mixtures of SPI and AP	6.70	38.30	22.10	32.90
SPI-CP conjugates (wet heating)	4.60	38.00	19.40	38.00
SPI-AP conjugates (wet heating)	4.41	37.68	19.21	38.70
SPI-CP conjugates (with ultrasound)	2.60	35.76	19.98	41.66
SPI-AP conjugates (with ultrasound)	3.70	35.97	20.37	39.96

Fig. 1

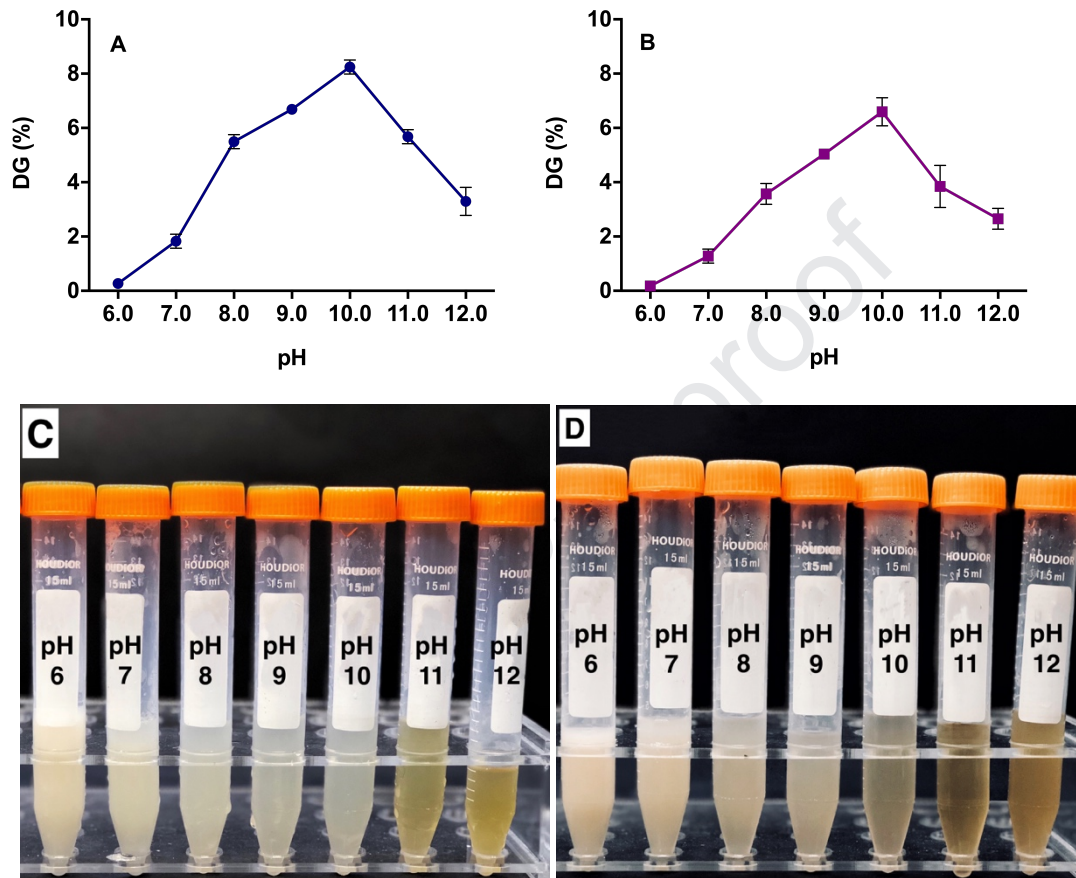




Fig. 2

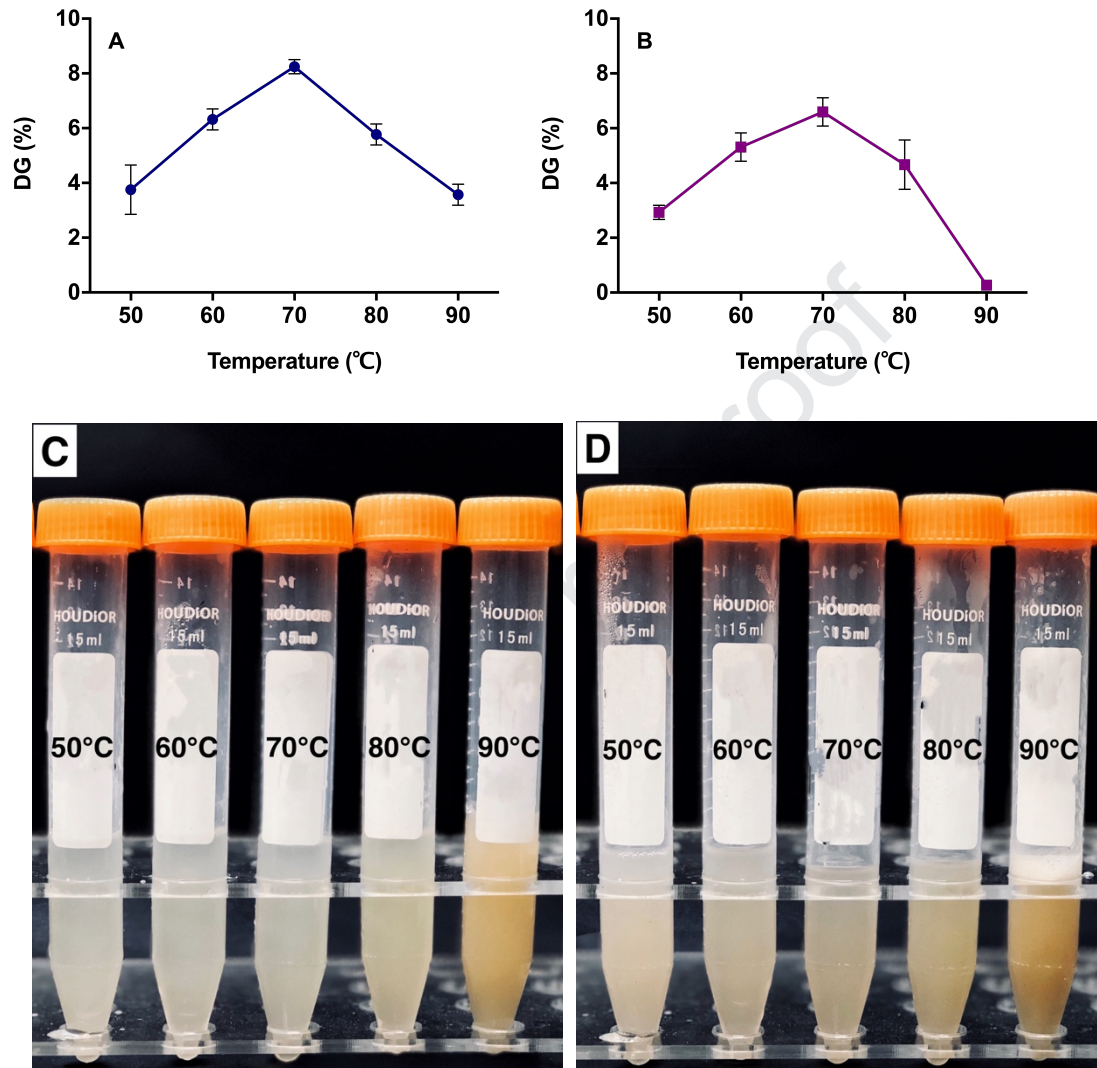


Fig. 3

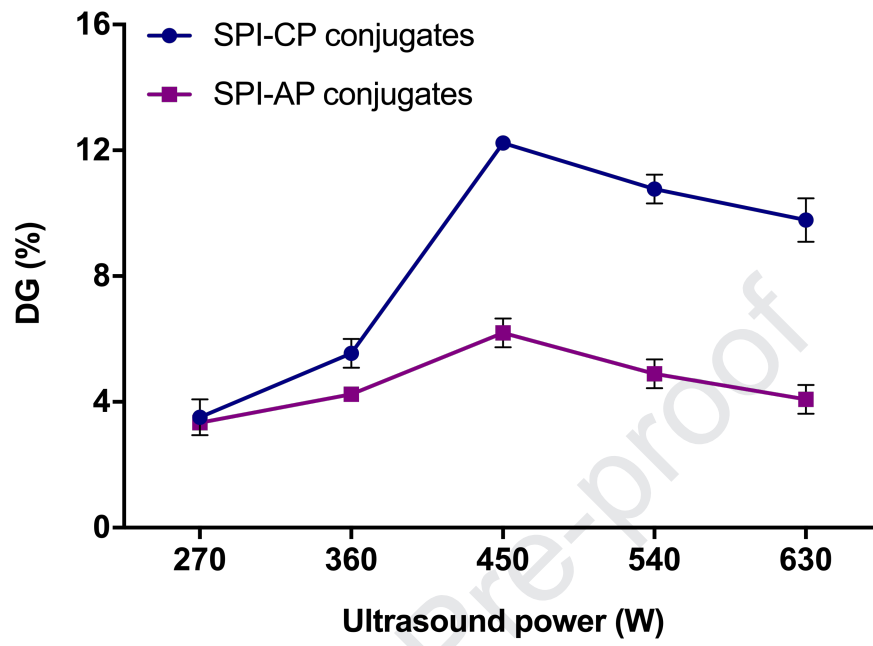
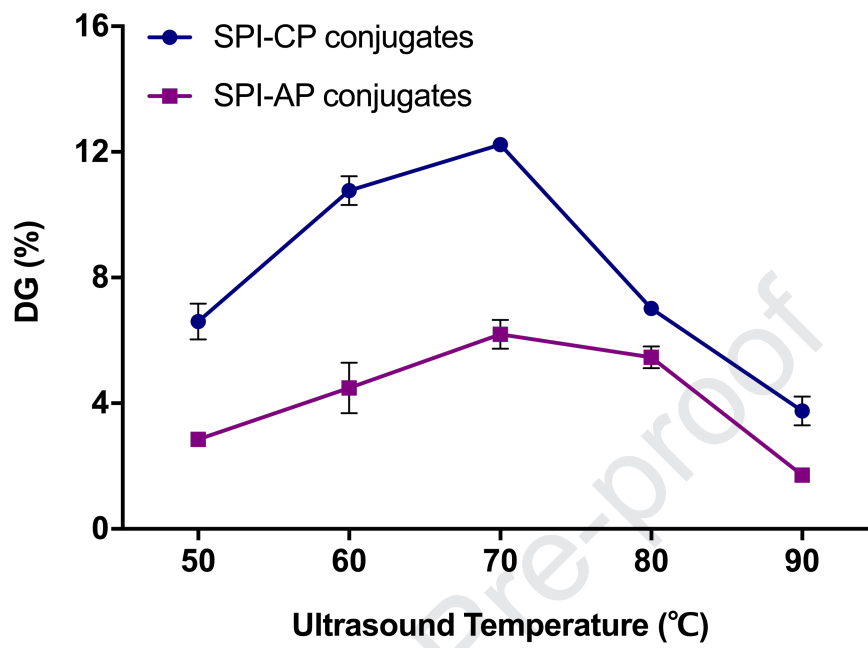
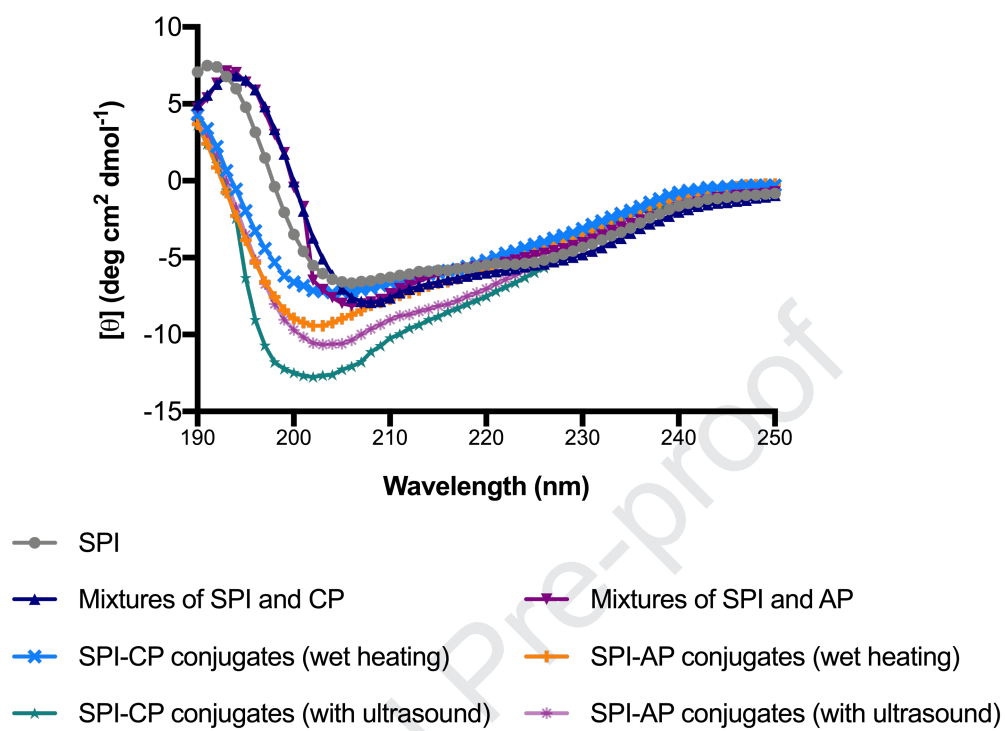


Fig. 4





**Fig. 6**

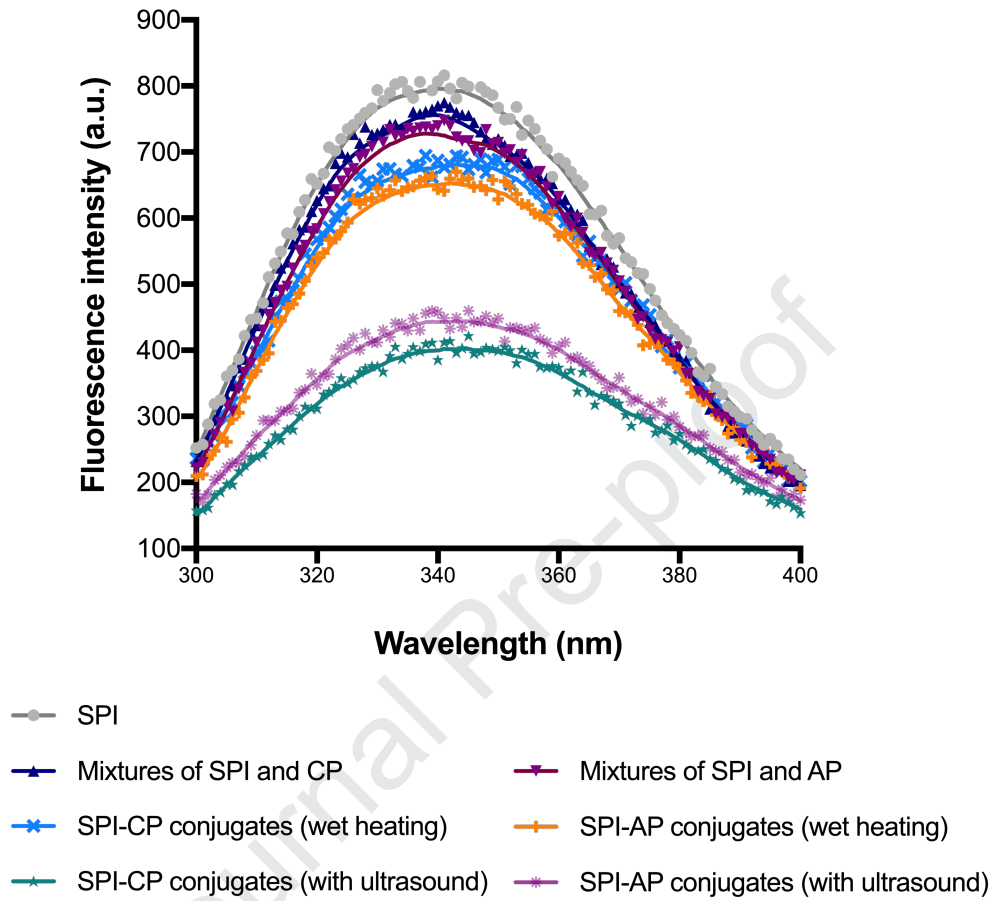
**Fig. 7**

Fig. 8

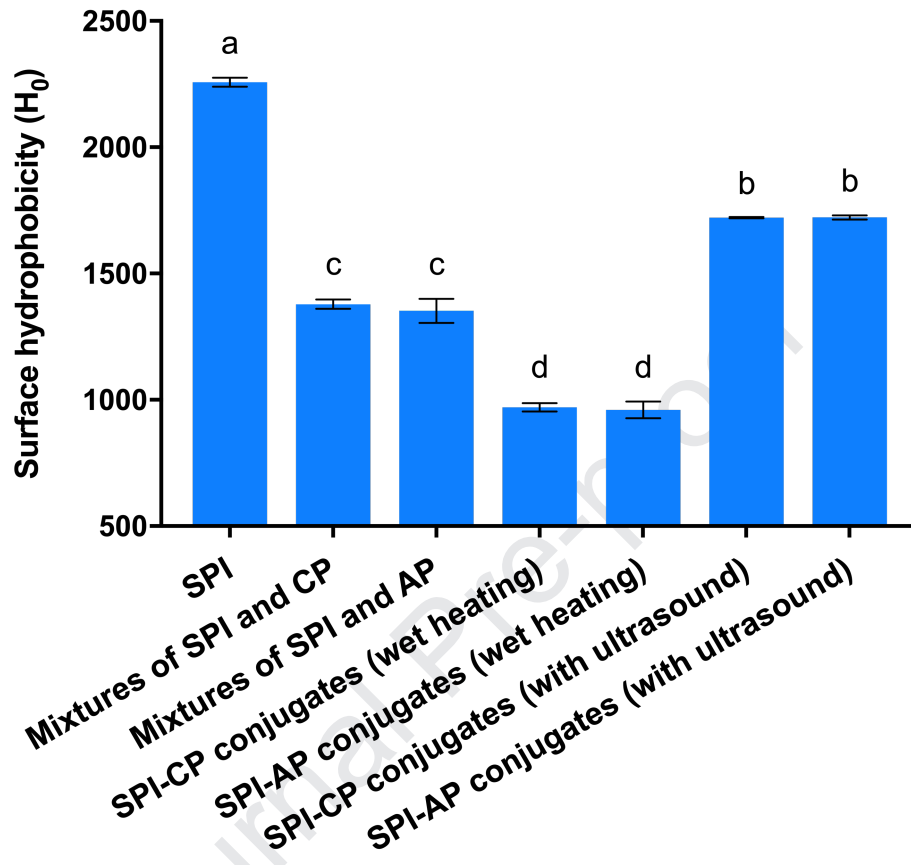
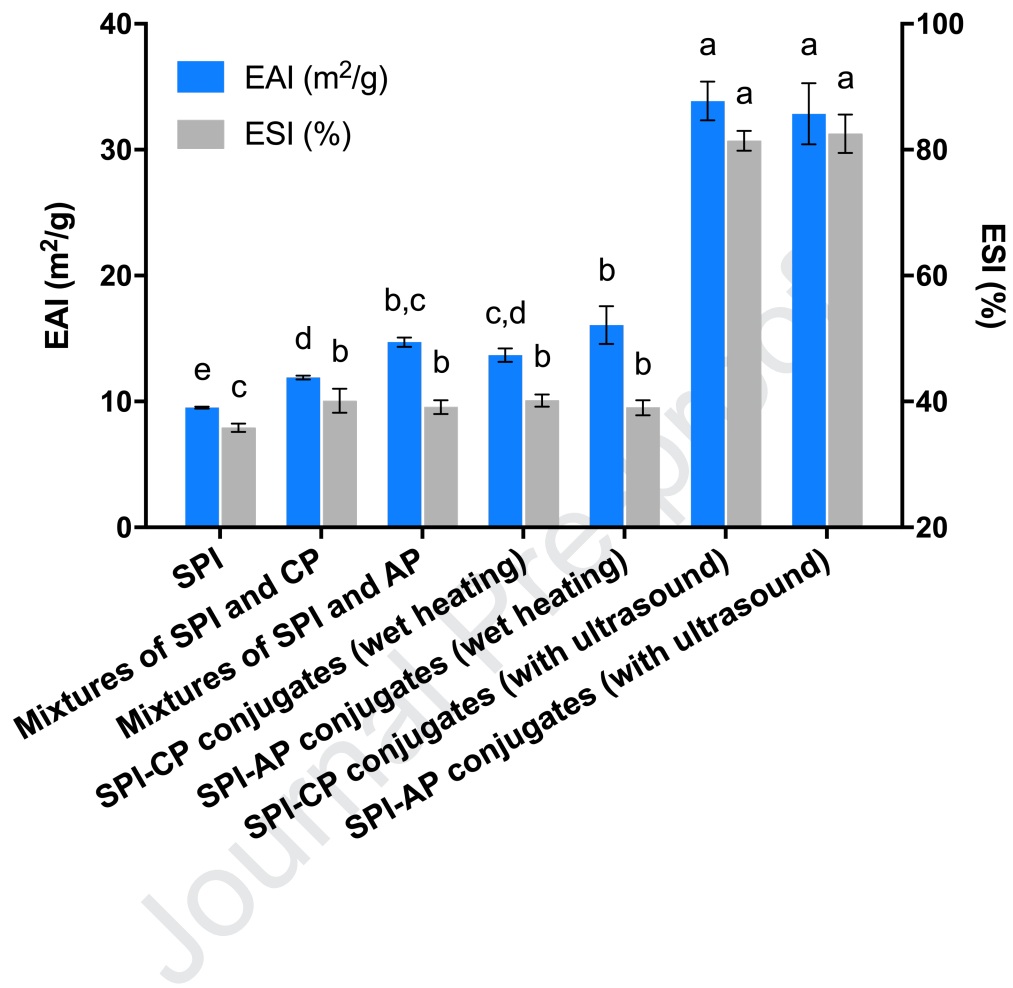


Fig. 9





## Highlights

1. Ultrasound enhanced the conjugation process resulting in higher grafting extents.
2. Formation of the conjugates was confirmed by SDS-PAGE analysis.
3. The ultrasound-assisted conjugation process led to looser protein structures.
4. Ultrasound increased the  $H_0$  and the emulsifying properties of the conjugates.
5. Both pectin samples are capable of forming excellent conjugates by ultrasound.

**Declaration of interests**

The authors declare that they have no known competing financial interests or personal relationships that could have appeared to influence the work reported in this paper.

The authors declare the following financial interests/personal relationships which may be considered as potential competing interests:

Journal Pre-proof